

Enhancing the Accuracy of Microwave Element Models by Artificial Neural Networks

Josef DOBEŠ, Ladislav POSPÍŠIL

Dept. of Radio Electronics, Czech Technical University, Technická 2, 166 27 Praha, Czech Republic

dobes@feld.cvut.cz, pospasil@jablotron.cz

Abstract. In the recent PSpice programs, five types of the GaAs FET model have been implemented. However, some of them are too sophisticated and therefore very difficult to measure and identify afterwards, especially the realistic model of Parker and Skellern. In the paper, simple enhancements of one of the classical models are proposed first. The resulting modification is usable for the accurate modeling of both GaAs FETs and pHEMTs. Moreover, its updated capacitance function can serve as an accurate representation of microwave varactors, which is also important. The precision of the updated models can be strongly enhanced using the artificial neural networks. In the paper, both using an exclusive neural network without an analytic model and cooperating a corrective neural network with the updated analytic model will be discussed. The accuracy of the analytic models, the models based on the exclusive neural network, and the models created as a combination of the updated analytic model and the corrective neural network will be compared.

Keywords

GaAs FET, pHEMT, microwave varactor, parameters extraction, CAD, artificial neural network.

1. Introduction

The Sussman-Fort, Hantgan, and Huang [1] model equations can be considered a good compromise between the complexity and accuracy (they are updated from [2]). However, both static and dynamic parts of the model equations must be modified when using them for possible pHEMT or varactor modeling (i.e., for the elements that are often used in the microwave circuits). All the model modifications defined below have been implemented into the program C.I.A. (Circuit Interactive Analyzer) [6]. However, the accuracy of the updated model functions is still of a percentage order. To be more precise, using the artificial neural networks is the effective and relative simple way because we can utilize the standard MATLAB toolbox [22]. There are two ways of using the neural networks. The first consists in approximating

the element by an exclusive neural network, the second combines the analytic model with a corrective neural network.

2. Improvement of the Analytic Model

The diagram of the GaAs FET model is shown in Fig. 1, which is applicable for all the PSpice modeling levels [16].

2.1 Modifying the Static Part of the GaAs FET Model

The fundamental voltage-controlled current source I_d of the GaAs FET model can be defined for the forward mode ($V_d \geq 0$) as

$$V_T = V_{T0} \boxed{-\sigma V_d}, \quad (1a)$$

$$I_d = \begin{cases} 0 & \text{for } V_g \leq V_T, \\ \beta (V_g - V_T)^{n_2} (1 + \lambda V_d) \tanh(\alpha V_d) & \text{otherwise,} \end{cases} \quad (1b)$$

and by the mirrored equations for the reverse mode ($V_d < 0$)

$$V_T = V_{T0} \boxed{+\sigma V_d}, \quad (2a)$$

$$I_d = \begin{cases} 0 & \text{for } V'_g \leq V_T, \\ \beta (V'_g - V_T)^{n_2} (1 - \lambda V_d) \tanh(\alpha V_d) & \text{otherwise,} \end{cases} \quad (2b)$$

where $V'_g = V_g - V_d$ – see the current and voltages in Fig. 1.

The model parameters V_{T0} , β , n_2 , λ and α have already been defined in [1], the parameter σ used in the “boxed” parts of (1) and (2) represents the update of the simpler classical models. Note that the Parker-Skellern realistic model contains similar relations [3] as a part of complicated internal functions – (1a) and (2a) can be considered as their core.

Although the equations (1) and (2) are relatively very simple, they contain an improvement in comparison with the classical Curtice model [2] (n_2 which characterizes gate voltage influence on I_d more precisely), and also in comparison with the classical Statz model [4] (σ which characterizes drain voltage influence on I_d more precisely).

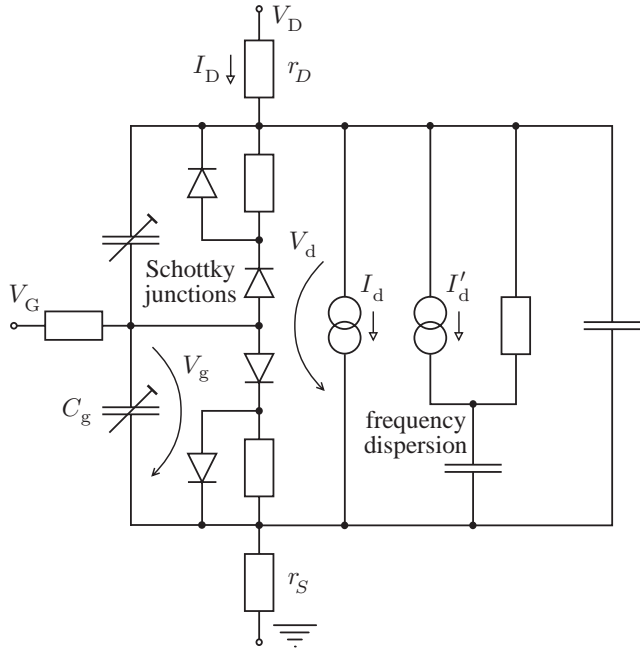


Fig. 1. Simplified diagram of the GaAs FET model, which includes the frequency dispersion. For characterizing a gate delay, a new method based on the second-order Bessel function (in frequency domain) and differential equation associated to that function (in time domain) is suggested in [7] (it uses the way proposed in [8], but with more precise modeling the delay).

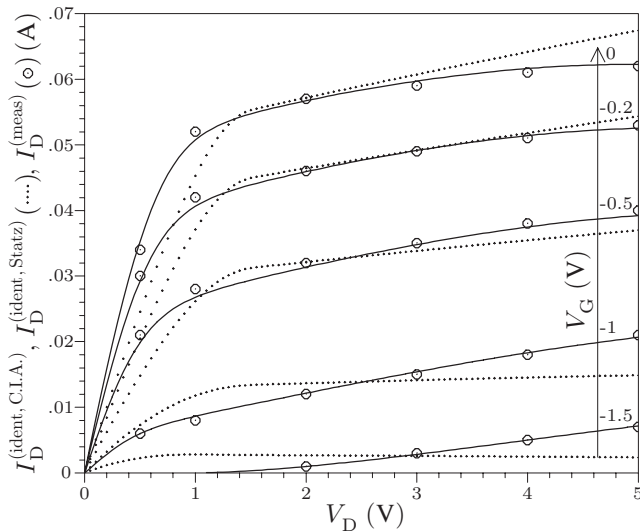


Fig. 2. Comparison of the GaAs FET model identification utilizing (1) and (2) and the classical Statz equations [4] ($\text{rms} = 2.73\%$ and $\delta_{\max} = 8\%$ for the model suggested here). The measured data are taken from [5].

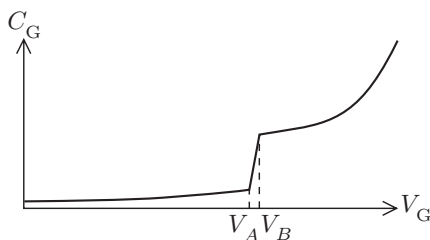


Fig. 3. Suggested GaAs FET model function for the varactor representation.

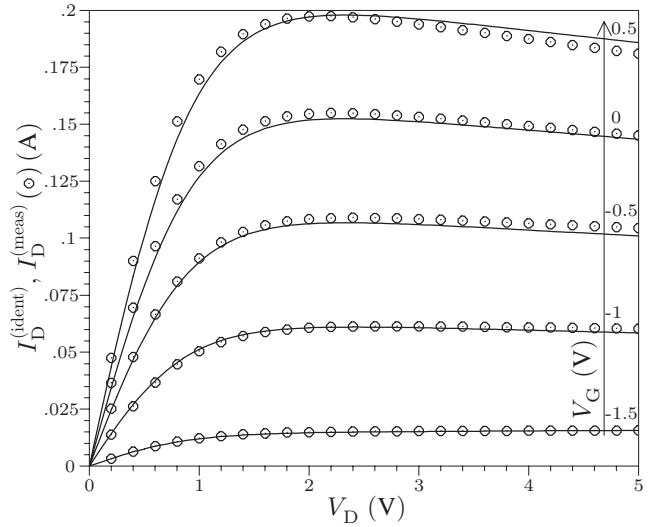


Fig. 4. Results of the pHEMT model identification utilizing (1) and (2) ($\text{rms} = 2.38\%$ and $\delta_{\max} = 8.24\%$). The measured data are taken from [9].

The importance of the modifications (1a) and (2a) can be clearly demonstrated by the identification of the model parameters for DZ71 [5] GaAs FET – see the results in Fig. 2 [18]. The C.I.A. optimization procedure [6] has provided the values of the model parameters $V_{T0} = -1.36\text{ V}$, $\beta = 0.0346\text{ A V}^{-2}$, $n_2 = 1.73$, $\lambda = -0.082\text{ V}^{-1}$ (note that the negative value of this parameter arises normally if σ is activated), $\alpha = 2.56$, $\sigma = 0.141$, $r_D = 2.88\ \Omega$, and $r_S = 2.62\ \Omega$ (note that the r_D and r_S parameters have already been estimated in [5]). To compare the achievement, the parameters of the same GaAs FET has also been identified by the classical Statz model [4]. As shown in Fig. 2, the model suggested here is more accurate, especially for the lesser values of the gate-source control voltage, and also for the greater values of the drain current.

2.2 Using the Modified Model as a pHEMT Representation

The modifications (1a) and (2a) also enable the model to be utilized for the pHEMT modeling – see the results in Fig. 4. The identification process has set the model parameters to $V_{T0} = -1.64\text{ V}$, $\beta = 0.102\text{ A V}^{-2}$, $n_2 = 0.991$, $\lambda = -0.0288\text{ V}^{-1}$, $\alpha = 1.16$, $\sigma = 0.00797$, $r_D = 0.3\ \Omega$, and $r_S = 0.2\ \Omega$. As seen in Fig. 4, the representation of pHEMT using (1) and (2) is very precise ($\text{rms} \approx 2\%$ only) and is slightly more accurate than the TriQuint one in [9] (see [10] and [11] as the exhaustive TriQuint model definitions). The model is also able to form a negative differential conductance, which is illustrated in Fig. 4. On the other hand, at very high frequencies, the s_{22} parameter does *not* match the DC curves. Therefore, a corrective current source I'_d must be added identified by the s parameters measurement. Note that embedding the frequency dispersion can also be performed in another more precise, but more complicated way, see [3].

2.3 Modifying the Dynamic Part of the GaAs FET Model

In general, the GaAs FET gate capacitance is highly nonlinear as shown in Fig. 3. Its definition splits into the three parts, similar to those in the Statz model [12, 13]

$$C_g = \begin{cases} \epsilon W \arctan \sqrt{\frac{\phi_0 - V_T}{V_T - V_g}} & \text{for } V_g \leq V_A, \\ \frac{V_g - V_A}{V_B - V_A} \left[C_{J0} \left(1 - \frac{V_B}{\phi_0} \right)^{-m} + \right. \\ \left. \pi \frac{\epsilon W}{2} - \epsilon W \arctan \sqrt{\frac{\phi_0 - V_T}{V_T - V_A}} \right] + \\ \epsilon W \arctan \sqrt{\frac{\phi_0 - V_T}{V_T - V_A}} & \text{for } V_g > V_A \wedge \\ & V_g < V_B, \\ \pi \frac{\epsilon W}{2} + C_{J0} \left(1 - \frac{V_g}{\phi_0} \right)^{-m} & \text{for } V_g \geq V_B, \end{cases} \quad (3)$$

where the transitional region is determined empirically [1]

$$V_A = V_T - 0.15 \text{ V}, \quad V_B = V_T + 0.08 \text{ V}. \quad (4)$$

All the model parameters have been defined in [1] with the exception of the “boxed” $-m$. This parameter can be found among the model parameters of the recent PSpice programs only, all the classical models always use the theoretical value $-\frac{1}{2}$ instead of $-m$ [4, 15].

2.4 Using the Modified Model as a Varactor Representation

The microwave varactors are highly nonlinear with observed dependencies similar to those in the GaAs FET gate capacitances. Therefore, the functions in (3) can be utilized after replacing C_g and V_g with the external ones, i.e., with C_G and V_G . Let's emphasize that such “empirical” method is often used in the GaAs FET modeling, especially in [3].

2.4.1 Testing the Varactors of Texas Instruments

Firstly, let's demonstrate this idea by identifying Texas Instruments EG8132 gate and source [14] varactors – see the results in Fig. 5 and 6. The identifications confirm that the usage of (3) enables more accurate approximation than the 6th order polynomial used by the authors of [14].

For the gate varactor, the optimization procedure has given the values of the model parameters $\epsilon W = 0.15711$ pF, $C_{J0} = 1.0771$ pF, $V_T = -2.7569$ V, $\phi_0 = 23.451$ V (!), and $m = 12.827$ (!). Of course, the last two parameters do not have “physical” values, which illustrates the necessity of using the general $-m$ -power in (3). From the physical point of view, the varactor is *not* defined for $V_G > V_B$ by the classical junction capacitance function – however, this formula is sufficiently flexible for approximating it.

For the source varactor, the optimization procedure of the C.I.A. has given the values of the model parameters

$\epsilon W = 0.13587$ pF, $C_{J0} = 0.66625$ pF, $V_T = -2.6026$ V, $\phi_0 = 13.251$ V, and $m = 8.1457$ with a more precise device characterization – let's compare the values rms and δ_{\max} .

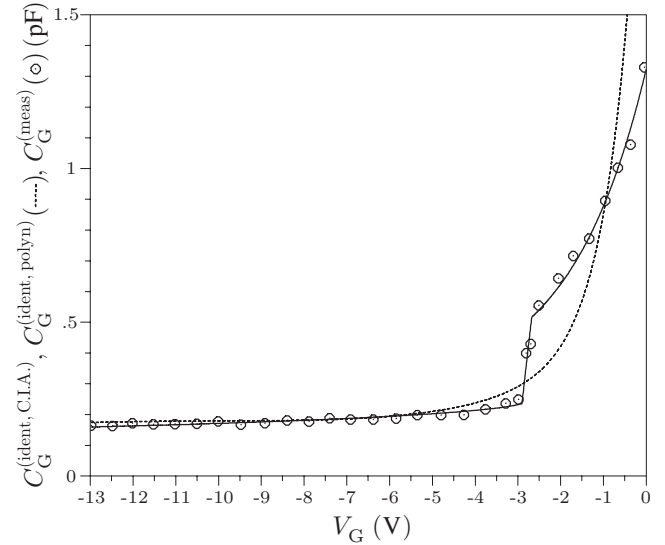


Fig. 5. Comparison of the EG8132 gate varactor model identification using (3) and the classical polynomial function (rms = 4.52% and $\delta_{\max} = 13.7\%$ for the model suggested here). The measured data are taken from [14], where the polynomial approximation $a_0 + a_2(V_G - V_a)^{-2} + a_3(V_G - V_a)^{-3} + \dots + a_6(V_G - V_a)^{-6}$ has also been tested with the inaccurate results (dashed curve) shown above (in [14], the parameters $V_a = -8$ V, $a_0 = -0.54$ pF, $a_2 = 2.3$ nF V², $a_3 = -87.938$ nF V³, $a_4 = 1.4$ μ F V⁴, $a_5 = -10.458$ μ F V⁵, and $a_6 = 30.48$ μ F V⁶ were used).

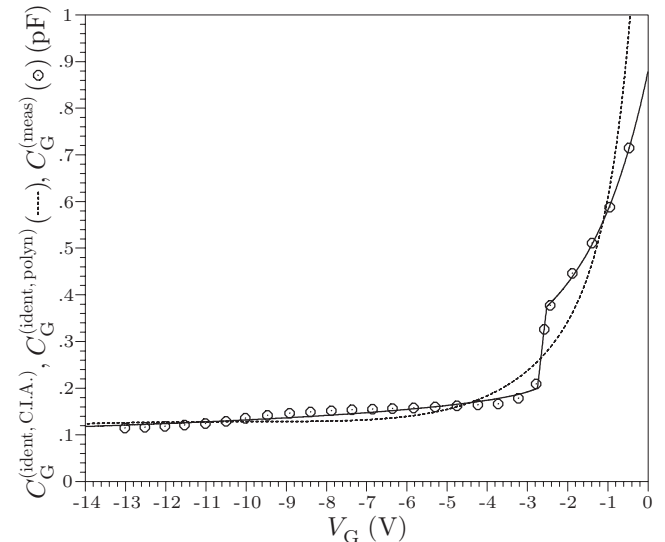


Fig. 6. Comparison of the EG8132 source varactor model identification using (3) and the classical polynomial function (rms = 4% and $\delta_{\max} = 6.87\%$ for the model suggested here). The measured data, and the polynomial approximation $a_0 + a_2(V_G - V_a)^{-2} + a_3(V_G - V_a)^{-3} + \dots + a_6(V_G - V_a)^{-6}$ are taken from [14] again ($V_a = -6$ V, $a_0 = -0.09$ pF, $a_2 = 0.4783$ nF V², $a_3 = -14.703$ nF V³, $a_4 = 0.18351$ μ F V⁴, $a_5 = -1.0475$ μ F V⁵, and $a_6 = 2.3177$ μ F V⁶ were used with the inaccurate results shown by the dashed curve).

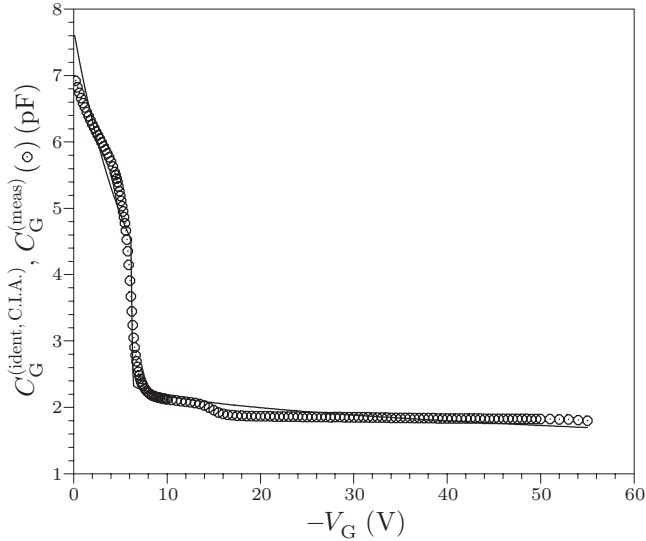


Fig. 7. Results of the ILC varactor model identification using (3) (rms = 6.21% and $\delta_{\max} = 23.7\%$). The measured data have been granted by the authors of [17].

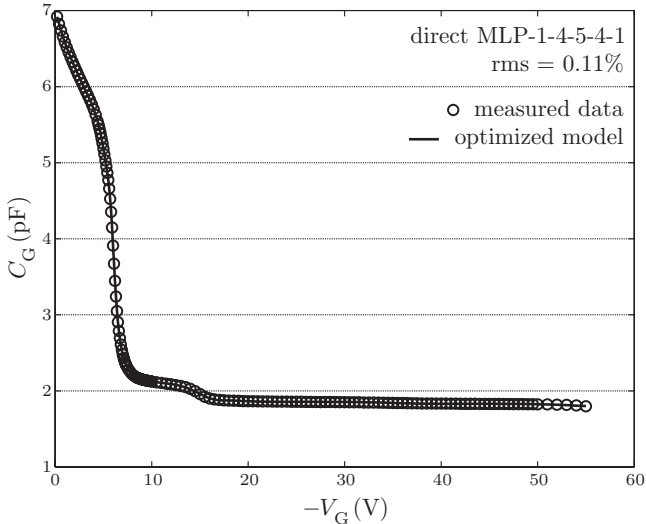


Fig. 8. Results of the ILC varactor model identification using the direct neural network ($\delta_{\max} = 0.4\%$ only!).

2.4.2 Testing the Varactor of International Laser Centre

Secondly, the highly nonlinear capacitance model [18] of the optical SACM APD layer structure MO457/4 [17] has been identified – see the results in Fig. 7. The optimization procedure of the C.I.A. program has given the values of the model parameters $\epsilon W = 1.51155$ pF, $C_{J0} = 5.30894$ pF, $V_T = -6.17455$ V, $\phi_0 = 204.491$ V, and $m = 30.4842$.

3. Improvement of the Models Using the Artificial Neural Networks

The root mean square deviations of the analytic models can be of the percentage order – it is clearly illustrated in Sec. 2. To obtain lesser values, the artificial neural networks are often used [19] for modeling the microwave elements.

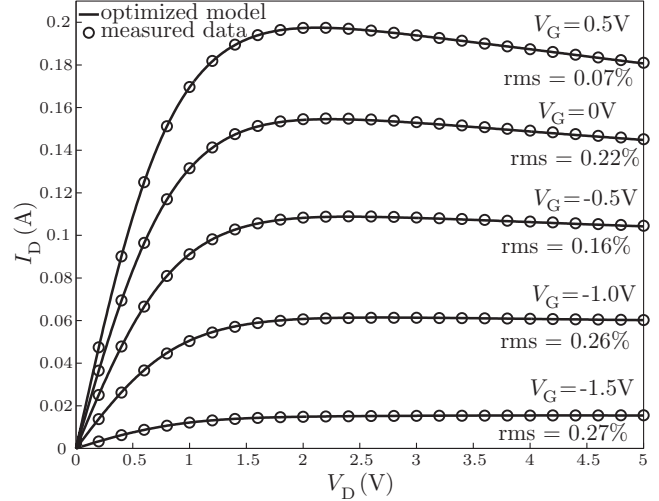


Fig. 9. Results of the pHEMT model identification using the direct neural network MLP-2-5-4-5-1 (rms = 0.2%).

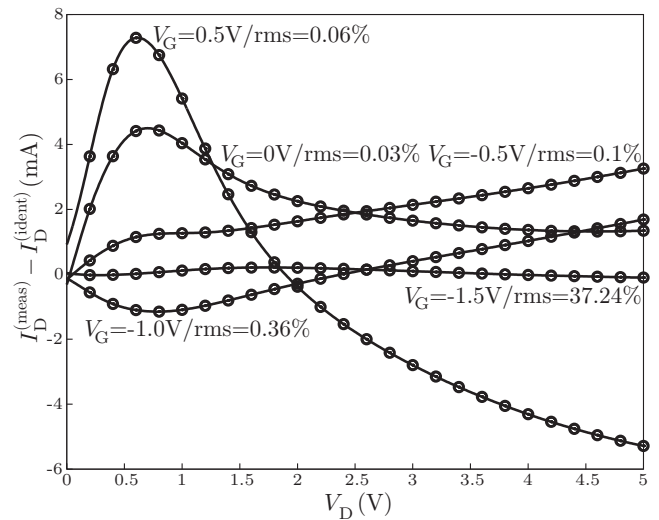


Fig. 10. Results of the identification of differences between the measured data and acquired analytical model shown in Fig. 4, which is an outcome of the corrective neural network MLP 2-8-10-6-1 (rms = 7.56%).

A detailed description of the conception of the neural networks can be found in [19] with the emphasis to modeling the nonlinear microwave elements. An especial conception of the *dynamic* neural networks (DNN) is defined in [20]. A brief description of the artificial neural network conception can also be found in [21].

There are two main ways for using the artificial neural networks. The first consists in utilizing an exclusive neural network, i.e., without an analytic model, and the second uses a neural network only as a correction tool of the difference between the measured data and identified analytic model.

3.1 Utilizing the “Direct” Neural Network

A neural network proposed for an approximation of an element without a cooperation with an analytic model can be

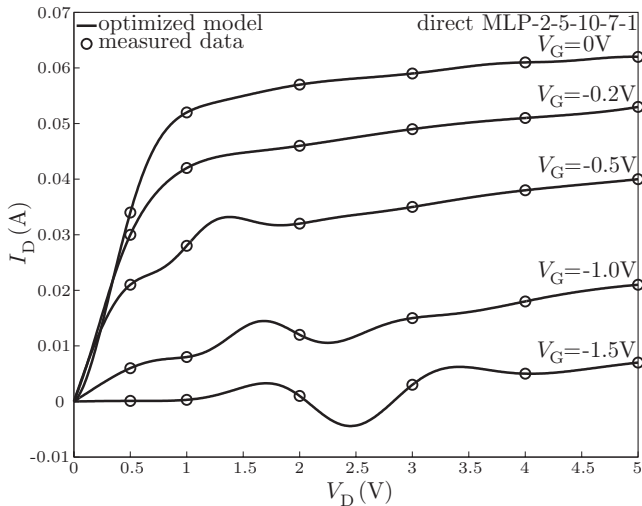


Fig. 11. Incorrect results of the GaAs FET model identification caused due to insufficient number of measured points.

marked as “direct”. Firstly, the microwave element models identified in Sec. 2 have been approximated using the direct neural networks to compare their precision with the updated analytic models. Regarding the neural networks, the standard multilayer structure [21, Fig. 1] has been used. The number of layers and the number of neurons in that layers have been carefully selected during many numerical tests. The MATLAB Neural Network Toolbox [22] has been used for all the numerical experiments.

3.1.1 Enhancing the Accuracy of the Varactor Model

The ILC varactor model has to be replaced by a neural network because the approximation with the analytic function (3) was not ideal – see Fig. 7 and the related values of rms and δ_{max} . For characterizing the varactor, a simple structure MLP-1-4-5-4-1 (including input/output layers) has been used with the results shown in Fig. 8 (MLP abbreviates Multi Layer Perceptron). Emphasize that the accuracy of this neural network is sufficient and hence there is no need to use a corrective neural network with the analytic model (3).

3.1.2 Enhancing the Accuracy of the pHEMT Model

The direct neural network has also been used for approximating pHEMT – see the results in Fig. 9 and Tab. 1.

V_G (V)	Analytic model	rms (%)	
		Direct	Corrective
0.5	3.23	0.07	0.00186
0	2.68	0.22	0.0007
-0.5	2.39	0.16	0.00206
-1	1.85	0.26	0.00696
-1.5	1.23	0.27	0.31
All	2.38	0.2	0.064

Tab. 1. Comparison of the accuracy of the acquired analytical model (Fig. 4) with the models created utilizing the direct (Fig. 9) and corrective (Fig. 10) neural networks.

Again, a relatively simple structure MLP-2-5-4-5-1 has been chosen. As shown in Tab. 1, the accuracy of the neural network has been approximately ten times better than the updated analytical model.

3.2 Utilizing the “Corrective” Neural Network

Secondly, a neural network can be used as a correction for the updated analytic model. In this case, only the difference between the measured data and previously identified analytic model is approximated using the neural network – such neural network can be marked as “corrective”. The accuracy of that method is expected to be greater in comparison with the direct neural network because only a relatively small value is approximated – see the example below.

3.2.1 Enhancing the Accuracy of the pHEMT Model

In Fig. 10, the difference between the pHEMT measured data and identified analytic model is shown and approximated using the corrective neural network. In this case, a slightly more complicated structure MLP-2-8-10-6-1 has been chosen. The resulting accuracy of the updated analytic model with the corrective neural network is shown in Tab. 1. It is clear that this methodology gives the best precision.

3.3 Limitations of Using the Neural Networks

The artificial neural networks must be used cautiously. As shown in Fig. 10, some curves do not include the point [0, 0] – therefore, this point must be added to the measured data before the optimization. Moreover, the element must be measured in a large number of points. Otherwise, we can obtain bizarre results as shown for the DZ71 GaAs FET in Fig. 11 – of course, the number of measured points of that GaAs FET is insufficient for the structure MLP-2-5-10-7-1.

4. Conclusion

A simple updating of the analytic model has been verified for the approximation of both GaAs FETs and pHEMTs with the precision of a percentage order. An unusual way is suggested for modeling the microwave varactors using the modified GaAs FET capacitance model function. Finally, using the direct and corrective neural networks is tested and compared from the point of view of accuracy. All the model parameters can be easily identified from measured data.

Acknowledgements

This paper has been supported by the Grant of the European Commission TARGET (Top Amplifier Research Groups in a European Teamwork), and by the Czech Technical University Research Project MSM 212300014.

Appendix

The root mean square and maximum deviations computed for the results in Figs. 2–10 are defined in the natural way

$$\text{rms} = \sqrt{\frac{\sum_{i=1}^{n_p} \left(\frac{y_i^{(\text{ident})} - y_i^{(\text{meas})}}{y_i^{(\text{meas})}} \right)^2}{n_p}} \times 100\%,$$

$$\delta_{\max} = \max_{i=1}^{n_p} \left| \frac{y_i^{(\text{ident})} - y_i^{(\text{meas})}}{y_i^{(\text{meas})}} \right| \times 100\%,$$

respectively, where $y_i^{(\text{ident})}$ and $y_i^{(\text{meas})}$ are the identified and measured values, and n_p is the number of all points.

References

- [1] SUSSMAN-FORT, S. E., HANTGAN, J. C., HUANG, F. L. A SPICE model for enhancement- and depletion-mode GaAs FET's. *IEEE Transactions on Microwave Theory and Techniques*, 1986, vol. 34, no. 11, p. 1115 – 1119.
- [2] CURTICE, W. R. GaAs MESFET modeling and nonlinear CAD. *IEEE Transactions on Microwave Theory and Techniques*, 1988, vol. 36, no. 2, p. 220 – 230.
- [3] PARKER, A. E., SKELLERN, D. J. A realistic large-signal MESFET model for SPICE. *IEEE Transactions on Microwave Theory and Techniques*, 1997, vol. 45, no. 9, p. 1563 – 1571.
- [4] STATZ, H., NEWMAN, P., SMITH, I. W., PUCCEL, R. A., HAUS, H. A. GaAs FET device and circuit simulation in SPICE. *IEEE Transactions on Electron Devices*, 1987, vol. 34, no. 2, p. 160 – 169.
- [5] JASTRZEBSKI, A. K. Non-linear MESFET modeling. In *Proceedings of the 17th European Microwave Conference EuMC*, 1987, p. 599 – 604.
- [6] DOBEŠ, J. C.I.A.—a comprehensive CAD tool for analog, RF, and microwave IC's. In *Proceedings of the 8th IEEE International Symposium on High Performance Electron Devices for Microwave and Optoelectronic Applications EDMO*, Glasgow (UK), 2000, p. 212 – 217.
- [7] DOBEŠ, J. Expressing the MESFET and transmission line delays using Bessel function. In *Proceedings of the 16th European Conference on Circuit Theory and Design*, Kraków (Poland), 2003, p. 169 – 172.
- [8] MADJAR, A. A fully analytical AC large-signal model of the GaAs MESFET for nonlinear network analysis and design. *IEEE Transactions on Microwave Theory and Techniques*, 1988, vol. 36, no. 1, p. 61 – 67.
- [9] CAO, J., WANG, X., LIN, F., NAKAMURA, H., SINGH, R. An empirical pHEMT model and its verification in PCS CDMA system. In *Proceedings of the 29th European Microwave Conference EuMC*, Munich (Germany), 1999, p. 205 – 208.
- [10] McCAMANT, A. J., McCORMACK, G. D., SMITH, D. H. An improved GaAs MESFET model for SPICE. *IEEE Transactions on Microwave Theory and Techniques*, 1990, vol. 38, no. 6, p. 822 – 824.
- [11] SMITH, D. H. *An improved model for GaAs MESFETs*. Technical Report. TriQuint Semiconductors Corporation, 2000.
- [12] MASSOBRIO, G., ANTOGNETTI, P. *Semiconductor device modeling with SPICE*. New York: McGraw-Hill, 1993.
- [13] SIJERICIĆ, E., PEJCIHOVIĆ, B. Comparison of non-linear MESFET models. In *Proceedings of the 9th International Conference on Electronics, Circuits and Systems ICECS*, Dubrovnik (Croatia), 2002, p. 1187 – 1190.
- [14] CHANG, C.-R., STEER, B. R., MARTIN, S., REESE, E. Computer-aided analysis of free-running microwave oscillators. *IEEE Transactions on Microwave Theory and Techniques*, 1991, vol. 39, no. 10, p. 1735 – 1744.
- [15] WONG, S. C. *WinSPICE manual*. Version 1.01. Hong Kong: The Polytechnic University, Dept. of Electronic Engineering, 2000.
- [16] *PSpice A/D reference guide*. Version 10.0. San Jose: Cadence Design Systems, Inc., 2003.
- [17] KLASOVITÝ, M., HAŠKO, D., TOMÁŠKA, M., UHEREK, F. Characterization of avalanche photodiode properties in frequency domain. In *Proceedings of the 5th Scientific Conference on Electrical Engineering & Information Technology*, Bratislava (Slovakia), 2002, p. 63 – 65.
- [18] DOBEŠ, J. Using modified GaAs FET model functions for the accurate representation of PHEMTs and varactors. In *Proceedings of the 12th IEEE Mediterranean Electrotechnical Conference*, Dubrovnik (Croatia), 2004, p. 35 – 38.
- [19] ZHANG, Q. J., GUPTA, K. C. *Neural networks for RF and microwave design*. Boston: Artech House, 2000.
- [20] XU, J., YAGOUB, M. C. E., DING, R., ZHANG, Q.-J. Neural-based dynamic modeling of nonlinear microwave circuits. *IEEE Transactions on Microwave Theory and Techniques*, 2002, vol. 50, no. 12, p. 2769 – 2780.
- [21] RAIDA, Z., LUKEŠ, Z., OTEVŘEL, V. Modeling broadband microwave structures by artificial neural networks. *Radioengineering*, 2004, vol. 13, no. 2, p. 3 – 11.
- [22] DEMUTH, H., BEALE, M. *Neural network toolbox for use with Matlab: User's guide*. Version 4. Natick: The MathWorks, Inc., 2000.

About Authors...

Josef DOBEŠ received the Ph.D. degree in microelectronics at the Czech Technical University in Prague in 1986. From 1986 to 1992, he was a researcher of the TESLA Research Institute, where he performed analyses on algorithms for CMOS Technology Simulators. Currently, he works at the Department of Radio Electronics of the Czech Technical University in Prague. His research interests include the physical modeling of radio electronic circuit elements, especially RF and microwave transistors and transmission lines, creating or improving special algorithms for the circuit analysis and optimization, such as time- and frequency-domain sensitivity, poles-zeros or steady-state analyses, and creating a comprehensive CAD tool for the analysis and optimization of RF and microwave circuits.

Ladislav POSPÍŠIL was born in 1971. He received his M.Sc. degree in electrical engineering from the Czech Technical University in Prague in 2004. Currently he works as technician at the Jablotron Ltd., Research and Developed Department, Section High Frequency. His research interests mainly consist in the active component modeling with the utilization of neural networks for microwave applications.